

Review

Processes of Physical Treatment of Stainless Steels Obtained by Additive Manufacturing

Artem Babaev ^{1,2}, Vladimir Promakhov ^{1,2,*}, Nikita Schulz ¹, Artem Semenov ¹, Vladislav Bakhmat ¹ and Alexander Vorozhtsov ¹

¹ Scientific and Educational Center “Additive Technologies”, National Research Tomsk State University, Lenin Avenue, 36, 634050 Tomsk, Russia

² “Nova-Health” Limited Liability Company, St. Visotsky, 28/7, 634040 Tomsk, Russia

* Correspondence: vvpromakhov@mail.ru

Abstract: With a vista of available stainless steel grades at our disposal, it is possible to manufacture items for a wide range of industries. These include chemicals production, medicine, and pharmacology, aerospace, power engineering, etc. Stainless steels are widely used mostly due to their unique property set, both mechanical and physicochemical ones, achieved by alloying various components. Stainless steel workpieces are usually obtained by melting, alloying, casting, and subsequent rolling to the desired shape. The experience in the study of the microstructure and processes of physical treatment of steel accumulated to the present day mainly concerns the machinability (blade, abrasive, laser, etc.) of such steels obtained by conventional techniques. Meanwhile, approaches to the production of workpieces from stainless steels by additive manufacturing (AM) methods are actively developing. In their turn, additive manufacturing technologies allow for producing workpieces that are structurally as close as possible to the final product shape. However, the use of AM workpieces in the manufacturing of functional products brings questions related to the study of the treatability of such steels by mechanical and physical processes to achieve a wide range of functional characteristics. This article discusses the issues of treatability and the characteristics and properties of stainless steels obtained by AM.

Keywords: additive manufacturing; stainless steels; mechanical and physical treatment



Citation: Babaev, A.; Promakhov, V.; Schulz, N.; Semenov, A.; Bakhmat, V.; Vorozhtsov, A. Processes of Physical Treatment of Stainless Steels Obtained by Additive Manufacturing. *Metals* **2022**, *12*, 1449. <https://doi.org/10.3390/met12091449>

Academic Editor: Kyriakos I. Kourousis

Received: 13 July 2022

Accepted: 25 August 2022

Published: 30 August 2022

Publisher’s Note: MDPI stays neutral with regard to jurisdictional claims in published maps and institutional affiliations.



Copyright: © 2022 by the authors. Licensee MDPI, Basel, Switzerland. This article is an open access article distributed under the terms and conditions of the Creative Commons Attribution (CC BY) license (<https://creativecommons.org/licenses/by/4.0/>).

1. Introduction

The onset of the use of additive manufacturing technologies in the production of workpieces from stainless steels has led to many issues pertinent to the processes of subsequent treatment of such materials [1–29]. Specifically, this is evidenced by both the growth in the number of scientific publications and the growing interest of the real economy in such products [10,13,19,30–37]. Some time ago, the use of AM consisted mainly in creating prototype parts that could not provide for a set of required physical and mechanical characteristics while only recreating a similar shape. As production technologies improved, it became possible to produce workpieces and usable items, but they required various post-processing techniques. The practical benefit of the use of additive technologies on engineered items is mostly related to the creation of design shapes that were previously inaccessible with conventional technologies as well as saving material that goes into production waste (shavings) during conventional treatment [5]. In such a conventional treatment process such as blade cutting, product shaping is performed by removing excess material from the workpiece to ensure the required geometry and surface quality. Alternative AM processes create three-dimensional (3D) workpieces incrementally by adding layers of materials. With this approach, the material utilization factor may exceed 0.75–0.85. Equipment used in the implementation of AM technologies has its own peculiarities. The entire process of creating workpiece object from a digital model is normally controlled by special software, and

process transitions are controlled by a microcontroller. To make movements in a coordinate system, both motors implementing linear displacements and multi-axis industrial robotic manipulators can be used [38,39].

As of today, the main area of application of AM is the production of functional products for aerospace and automotive industries [1,31,35,40,41], biomedicine [8,12,16,17,42], chemical and energy industries [30] as well as manufacturing press equipment [25,43–45], electronic devices and measuring instruments [46]. Dedicated studies are devoted to the use of AM in the production of jewelry [47] and cutting tools [15,48]. The latter may include fuel engine injectors, atomizers, components of ejector, and spray units. Much attention is paid to the creation of parts that cannot be obtained by casting or cutting. Examples of such products are various lattice structures [27,49] and thin-walled products [50]: liquid and gas mixing chambers with functionally developed internal geometry, apertures, and cavities of cooling modules, etc. The real economy initiates research on the use of combined AM technologies (deposition and subsequent treatment) for the repair and restoration of functional items [19,39,51].

AM processes use materials such as powder [18,20,52–63], wire [6,26,34,64–66], or sheets as raw stock, and the creation of layered connections is realized through exposure to a certain source of energy, followed by melting and crystallization. Also, the so-called feedstock using inkjet printing technology is sometimes used [39,67], see in Figure 1.

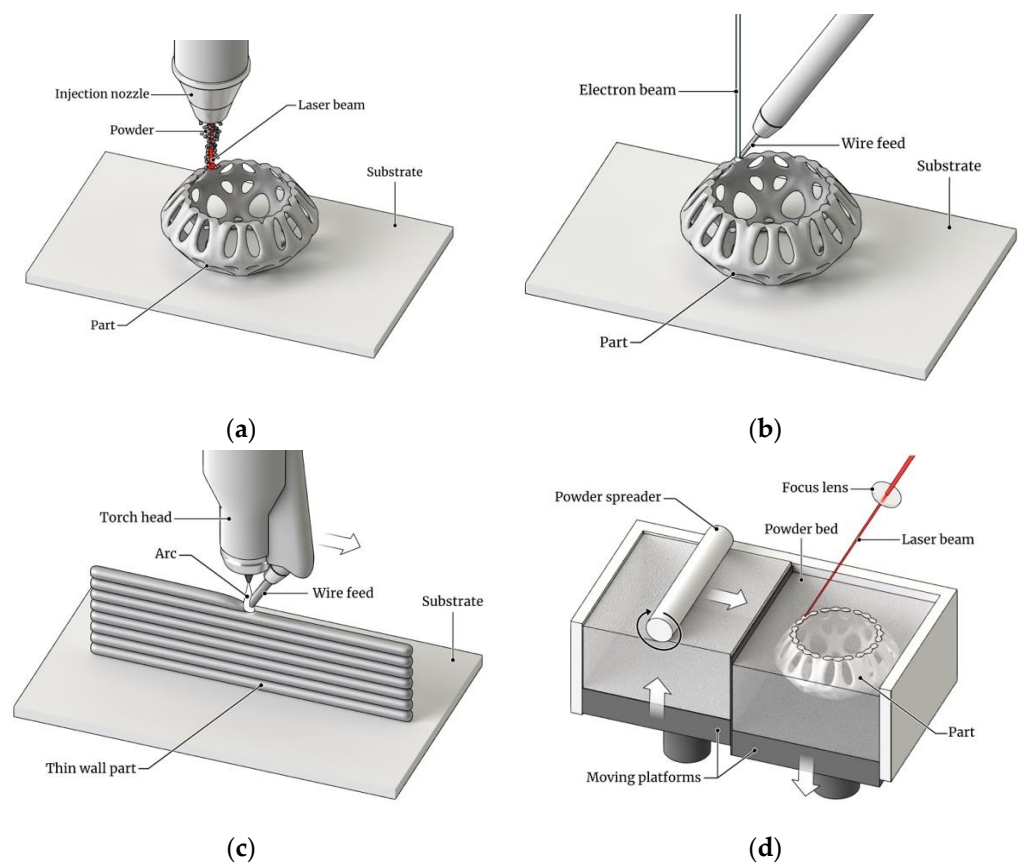


Figure 1. Illustrations and a schematic representation of AM techniques depending on the item deposition process, the source of thermal energy, and the form of the rawstock (a) is laser L, (b) is electron beam EB, (c) is wire feeding, electron arc sintering (PA), (d) is powder bed fusion.

AM processes fall into two categories defined by ASTM F2792 [68] as Directed Energy Deposition (DED) and Powder Bed Fusion (PBF). Another difference is the type of thermal energy supply source [69]. As the latter, a laser (Laser-L) [3,11,15,22–27,36,40,52,70–78], an

electron beam (EB) [39,69,79–81], plasma arc (PA) [82,83] and gas metal arc (GMA) [84–86] are used.

The choice of a certain AM technique requires a preliminary analysis of the design of the item of manufacturing, raw materials, and target physical and mechanical characteristics. However, using any of the above methods entails processes of removal of workpiece supports [87,88] and subsequent post-processing to give the item certain dimensional accuracy [7,89], surface layer quality and surface properties.

Recently, stainless steels have been quite often used as structural stainless steel in AM. There is a pronounced tendency among researchers to choose steel grade 316L. According to ASTM A240 [90], this steel belongs to the group of chromium- and nickel-chromium, chromium- and manganese-nickel stainless steels. 316L steel is a structural cryogenic austenitic steel. This steel is resistant to corrosion in aggressive environments and to most external atmospheric effects including cryogenic exposure. 316L steel tends to maintain structural integrity at increasing and decreasing temperatures. Thanks to the low carbon content of 316L steel, it is well suited for the fabrication of welded structures. Molybdenum in the composition protects 316L steel from decay in salty sea water, vapors of CH₃COOH acid, and other aggressive environments. An alloy of iron and chromium forms a protective layer on the surface of 316L steel that is resistant to mechanical and chemical stress. The chemical composition of 316L steel and some basic mechanical properties are shown in Tables 1 and 2, respectively.

Table 1. Chemical composition of 316L steel in % data from [4,9,16].

C	Mn	P	S	Si	Cr	Ni	Mo	Ti	Fr
<0.3	<2.0	<0.045	<0.03	<1.0	16.0–18.0	10.0–14.0	2.0–3.0	<0.5	The rest

Table 2. Some basic mechanical properties of 316L steel, data from [16,23,28,72].

Tensile Strength, MPa	530 ... 640
Yield strength at 0.2%, MPa	290 ... 295
Brinell hardness, HB	165 ... 230
Fatigue strength, N/mm ²	220 ... 260
Relative elongation, %	40 ... 42

Also, the use of 18Ni steel (maraging steel) for AM research is observed. This steel features high tensile strength, hardness, and fracture toughness. At the same time, it retains good ductility and impact strength due to the solubility of Ni, Ti, and Mo in the matrix martensite after aging treatment. Particles can strongly hamper the movement of dislocations to increase the strength of maraging steel. Due to improved thermal conductivity, and low thermal deformation, maraging steel is widely used in the aerospace industry, in the manufacturing of precision elements of mechanical transmissions, as well as molds and other mission-critical products. The chemical composition of 18Ni steel and some basic mechanical properties are shown in Tables 3 and 4, respectively.

Table 3. Chemical composition of 18Ni steel in %, data from [91].

C	Mn	P	S	Si	Cr	Ni	Mo	Co	Ti	Fr
<0.01	<0.06	<0.01	<0.01	<0.02	<0.1	17.0–19.0	4.0–5.0	7.0–8.0	<0.5	The rest

Table 4. Some basic mechanical properties of 18Ni steel, data from [91].

Tensile Strength, MPa	1500 ... 1750	1034
Yield strength at 0.2%, MPa	760 ... 810	758
Brinell hardness, HB	300 ... 330	304
Modulus of Elasticity, GPa	190 ... 200	190
Relative elongation, %	12 ... 18	18

Research of stainless steels manufactured by AM processes covers the processes and mechanisms of crystal growth [92–94], the study of the effect of AM process variables on physical and mechanical properties [45,52,70,71,75], optimization of growth processes, and comparison of the microstructure of steels depending on various AM processes [94]. Also, there are studies dedicated to the optimization of layer-by-layer deposition [36,55,71,95], study of microstructure, microhardness [16,36], tensile strength [91], impact strength [64] and the influence of process variables and heat treatment of steel [2,3,37,44,45,58,60–63,70,71,80–83,95].

2. Investigated Characteristics in Post-Processing

The obvious advantages of using additive manufacturing processes for producing workpieces from stainless steels prevent the grown part from being used immediately as final product [96]. A critical disadvantage here is that the surface quality and its functional characteristics are much worse as compared to machined or polished parts obtained from a workpiece produced by conventional processes. Let us consider some of the parameters, control over which is investigated in a number of publications.

2.1. Roughness

Object surface has a characteristic that often has critical values in the case of AM-produced items, and it prevents their use as final functional products. This characteristic is complex, and it is called roughness [56,79,80]. Roughness combines a large number of different parameters including amplitude, distance as well as hybrid parameters. Control of surface roughness is very labor-intensive, but it is important for many fundamental problems, such as friction, contact deformation, thermal and electrical conductivity, ensuring the tightness of contact joints, as well as positioning accuracy.

The actual microgeometry of the surface is quite complicated due to peculiar surface morphology after AM and it often cannot be comprehensively described even by standardized roughness parameters.

However, engineering tasks do not require such exhaustive understanding. Despite a variety of standards (there are more than 60 of them) that regulate roughness, only a few have found wide engineering applications. Surface roughness and texture are determined both by technological processing parameters and by the properties of the material and the method of its production. The dependence of roughness on the above characteristics is discussed below. Particular attention is paid to the achieved roughness parameters depending on the treatment method used.

2.2. Microhardness, Fatigue Performance

The relative microhardness of such materials as metals or ceramics is determined by the depth to which a diamond-pyramid indenter penetrates. Microhardness plays a decisive role in the choice of material and the technology of its heat treatment in assessing the resistance to abrasive or mechanical wear. Meanwhile, fatigue performance is a major concern for mechanical components subjected to cyclic loading, especially where safety is paramount. The fatigue characteristics of manufactured parts largely depend on the integrity and roughness of their surface, since fatigue cracks usually originate in the so-called stress concentrators.

Thermal treatment can change the microstructure, phase composition and therefore physico-mechanical properties of stainless steels. Such thermal treatment techniques as artificial aging, annealing, and normalization on AM-fabricated workpieces cause noticeable changes in microhardness. Thus, article [70] provides data on the effect of physical treatment (artificial aging) on the microhardness of stainless steel, an increase from 381.2 to 645.9 HV. This translates into increased impact strength which results in increased resistance to cutting-edge machinability. In regards to changes in the microstructure, quick cooling during laser sintering of a powder leads to the emergence of martensite, which is shown in [2]. Martensite grains in the matrix increase their microhardness by ~31.53% as compared to hot rolled steel of similar chemical composition. However, this is accompanied by a negative process aspect: improved microhardness leads to increased cutting forces required for machining thereby reducing tool life. It was shown in [97] that heat treatment of chromium steel specimens has a beneficial effect on their strength but in some cases, it may lead to a decrease in ductility. Mechanical tests of AM-fabricated samples confirmed the statement about their usability for manufacturing functional products along with conventionally manufactured parts. However, porosity has to be controlled and kept to a minimum here.

As for research wherein stress and crack concentrators are studied, in [32] it is shown that there is a significant difference between polished and machined workpieces in regards to the formation of stress and crack concentrators. On the other hand, there are works [28] that report the use of thermal treatment for 316L grade steel whereby the identical intensity of development of growth of cracks in the microstructure is reported. As a result of the comparison of fatigue characteristics of an AM-fabricated and conventional steel, the authors highlight a rather insignificant difference in the numerical indicators. Structural strength and structure failure are related to the durability of individual parts and the reliability of the system in which the parts operate. Studies of the properties of AM-fabricated stainless steel workpieces as well as their destruction and strength parameters are regarded for different fabrication technologies. Article [64] describes mechanisms of destruction of specimens obtained by wire sintering technology and provides research results thereof. The authors point to the dominant effect of ductile fracture in the direction of welding where the thickness of the weld bead is the determining factor in the onset of fracture. During laser sintering, changes in the samples' static bending strength and cyclic axial loading before destruction are related to varying laser sintering regimes [93]. It is also shown in the above article that the creation of a cellular structure in the course of specimen growth results in the preservation of rigidity of the entire structural system. The influence of cavities (pores) inside the material and on its surface in the course of samples' growth reduces the cyclic strength and fatigue strength. Maximum density (i.e., one close to the theoretically estimated maximum) can be reached, for example, by laser sintering in the following regime: laser beam travel speed at 100 mm/s and hatch distance at 75 μm . The authors of [98] present data on the possibility of fabricating samples of different densities from 316L steel obtained in the process of selective laser sintering. Meanwhile, [16] suggests using post-processing to improve the cyclic strength and fatigue strength. The authors of [99] obtained similar results by manual mechanical polishing of AM-fabricated 316L steel to Ra 0.4 ... 0.1 μm with abrasive pastes applied to soft discs. This is related to a decreased overall area of the porous surface. The authors note that the behavior of AM-produced 316L steel during tension and fatigue strength tests does not differ from similar steel obtained by conventional casting provided that all other conditions are the same. Point laser hardening provides for an increase in the microhardness of 316L grade steel surface by 7–22% [24]. Such local laser hardening also contributed to an increase in the yield strength by 16%, while tensile strength remained virtually unchanged. The authors also show satisfactory convergence of the finite element model with the results of a full-scale experiment in terms of predicting mechanical characteristics. In the case of laser polishing of 316L steel, an increase in the tension strength is observed. This is caused by the elimination of defects that emerged during the sintering process as well as a decrease

in the size of microstructural grains. This is shown in [52] wherein the authors present data on an increase in the number of grains smaller than 10 μm and the density of dislocations at the boundaries of substructures.

2.3. Anisotropy, Residual Stresses

The quality of properties exhibited for different values when measured along axes in different directions. Anisotropy may affect mechanical properties by altering the conditions of the formation of microstructure and macrostructure of layers and those of the base material. Anisotropy in the properties of AM-fabricated materials is caused by peculiarities of the material microstructure and process-related aspects inherent to the growth of specimens. Thus, articles [71,72,95] show the effect of anisotropy of steel properties on microhardness. The studies and subsequent measurements were carried out on samples oriented horizontally, vertically, and at an angle of 45° relative to the direction of workpiece growth. Technically, this was achieved by fabricating required workpieces of ad-hoc structural forms. Here vertical orientation provides for the highest HV hardness even in the course of subsequent thermal treatment (artificial aging). Anisotropy of properties achieved in the course of workpiece orientation during deposition is also confirmed in [32]. Meanwhile, the authors observed changes in the fatigue characteristics of AM-fabricated 316L steels when their growth orientation was changed. Also, the anisotropy of properties can be lowered by adding thermal treatment, i.e., artificial aging. This is demonstrated in article [71]. However, it is noted that the growth direction and its influence on the anisotropy persist despite thermal treatment.

In [49], in the course of selective laser sintering of 316L steel specimens, the influence of the orientation (growth angle) of specimens on the formation of grain size is shown. Meanwhile, it was noted that the frequency at which large elongated grains emerge can be reduced on workpieces with a thickness of at least 0.4 mm. However, the authors point out that manufacturing and post-processing workpieces with a wall thickness of ~ 0.2 mm is technically feasible. In [20], the influence of the orientation of grown workpieces on the change in the texture (roughness) of the surface has been shown. Actual roughness values may differ by 0.4 . . . 69.3% depending on the subsequent machining used. In [37], the effect of the anisotropy of the properties of austenitic stainless steel on tensile strength and yield strength is shown. The orientation of samples during fusion leads to differing but uniform microhardness. Subsequent heat treatment, while removing residual stresses, adds inhomogeneity to the distribution of microhardness.

Superficial plastic deformation and strengthening promote increased residual compressive stresses in the superficial layers which result in an increase in the fatigue strength and mechanical characteristics within allowable limits. Data on the research of physico-mechanical characteristics of an AM-fabricated maraging steel subjected to shock hardening are provided in article [99]. Similar experimental conditions and results are observed during cutting-edge machining. Milling in [32] can be used as an example wherein an increase in the microhardness of maraging steel is observed, caused by the formation of residual compressive stresses in the superficial layer. The authors of [100] report an increase in the surface microhardness by 31.6% for samples of maraging steel obtained by a hybrid process: a combination of powder laser sintering and milling processes. Accordingly, milling of such samples is accompanied by an increase in cutting forces and hence faster tool wear due to dulling of the cutting edge. Using a combination of cold deposition and selective laser melting in [75], the authors could observe an increase in tensile strength and elastic toughness at fracture. For sample finishing, the authors used turning and reported satisfactory machinability of the workpieces.

2.4. Corrosion Resistance

Corrosion is the loss of metal to a reaction with the environment, and it is measured as the percentage of weight loss or as the penetration rate of corrosion over time [101]. Predicting the conditions and rate of corrosion is an important condition for choosing a

post-treatment process for AM-produced workpieces [102,103]. The use of cutting-edge and electrochemical techniques promotes the reduction of point (pitting) corrosion [104]. Article [9] shows how the use of electrochemical polishing on 316L steel obtained by laser deposition can reduce sensitivity to pitting thereby increasing resistance to the emergence of corrosion centers on a polished surface. Also, in article [33], the authors report the influence of a series of laser sintering parameters (for AM) and temperature gradient (for melting) as well the influence of microstructure characteristics and volumetric chemical microstructural inhomogeneities on local corrosion resistance. The authors emphasize that corrosion resistance can be improved not only by controlling these parameters but also by applying mechanical post-processing techniques. In [104], the authors study the effect of electrochemical polishing on a range of surface parameters of stainless steels among which corrosion resistance stands out. This is especially important in the treatment of items with complex inner surface that cannot be machined. The authors noted that electrochemical polishing reduces the likelihood of a chemical oxidation reaction followed by the formation of corrosion foci. In [105], tests for the corrosion resistance of AM-fabricated 316L steel were carried out using NaCl acid (3.5% wt.). The authors present the results highlighting that no difference was found in the formation of the oxide film for different directions of grain growth during solidification. It was found that during sintering, the passage of laser beam oriented at an angle of 90 degrees to the previous layer provides for the best performance in terms of corrosion resistance, and at 67.5 degrees, for the worst.

2.5. Biocompatibility

In article [12], the authors present data on the compatibility of orthopedic implants produced by AM. The production cycle is shown, including the processing of patient data and the creation and refinement of a digital model for the preparation of anatomical reconstruction. The authors also highlight the need for using finishing treatment technologies for such products. However, the authors point out that observation in the postoperative period is an important measure to increase the likelihood of biocompatibility. They propose growing a layer-by-layer gradient material structure during its deposition.

In article [106], the authors study the effect of electrochemical polishing of 316L steel on biocompatibility. They point out that a positive effect on the attachment of biological cells is achieved compared to an untreated surface. This opens the possibility of further usage of the polishing process for the fabrication of implants for various purposes. Article [17] presents results of studies of the usage of various combinations of post-processing on a 316L steel obtained by selective laser melting for biomedical applications. The authors used a sequence of the following processes: abrasive blasting, abrasive electropolishing, and finally, anodic electropolishing. It was found that after abrasive blasting with glass beads, the surface is impregnated, i.e., saturation of surface layers with particles of the processed material is taking place. Electropolishing further reduces roughness but it does not remove penetrated particles. This introduces a number of limitations and a need for further research on using such a process sequence for mission-critical medical devices.

2.6. Tribological Properties

Tribological properties are understood as a set of specific characteristics that build contact interaction of rubbing surfaces. Coefficient of friction is of the most interest and it is often related to surface roughness parameters. Article [96] describes the data on the change in friction coefficients for samples of a chromium-molybdenum-vanadium steel obtained by selective laser sintering from powder with particle sizes of 18–44 μm . In particular, the authors found that the use of abrasive grinding and subsequent polishing to Ra 0.15 reduces the coefficient of friction by more than 10 times as compared to a surface fabricated by 3D printing only. The minimal achieved friction coefficient was 0.01. The use of polishing followed by laser beam treatment leads to an increase in the friction coefficient from 0.1 to 0.13.

3. Methods of Treatment of Stainless Steel AM

Available scientific publications describing the application and research of various post-processing techniques used on AM-fabricated stainless steels relate that such parts show poor quality and irregular surface morphology. This drawback makes such parts inapplicable for further use in real mechanisms and machine designs without finishing. The surface irregularities are created by the process of layer-by-layer material deposition, melting, and solidification [56,81].

3.1. Machining Technologies

Machining is the technique most commonly used for altering the shape and quality of the surface of a workpiece fabricated by AM (see Figure 2). Machining comprises a wide range of technologies that combine directional material removal (overlap and outsize) with the formation of shavings and a new surface. Such a process of excess material removal is implemented on metal-cutting machines belonging to milling, turning, and grinding categories using cutting and abrasive tools: cutters, blades, and grinding wheels, respectively. Depending on the type of tool material and variations in the regimes and kinematics of treatment, different surface quality, and machining process performance can be achieved. The roughness achieved by machining AM-produced stainless steel workpieces is in the vicinity of R_a 0.2–1.6 μm and it depends on the chosen process and the treatment regimes [16,35,107]. In blade machining, such kinematic parameter as feed (the movement of the cutting edge of the tool relative to the workpiece per unit of time or per revolution of the tool or the workpiece) has a decisive influence on the surface roughness. This circumstance is typical both for workpieces obtained by AM and for conventional cast materials.

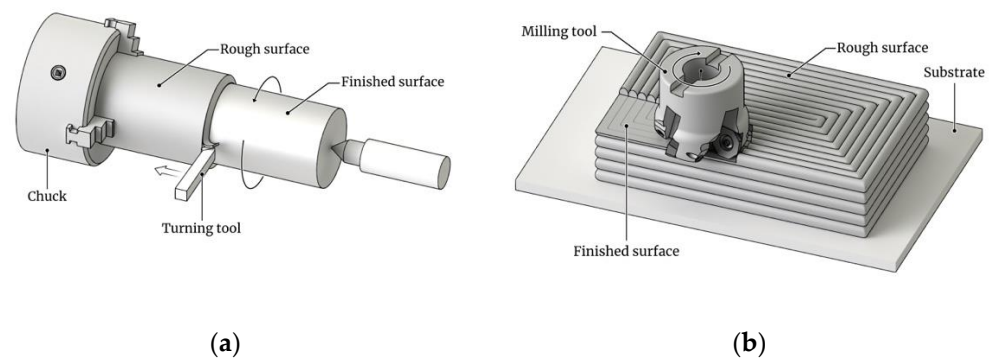


Figure 2. Blade machining processes implemented on metal-cutting machines: (a) is turning the outer cylindrical surface with a through cutter; (b) is milling the outer plane with a face mill.

Article [65] studies the process of milling thin-walled parts with a carbide tool whereby the parts had been obtained from nickel steel by wire-arc growth. The authors noted that an increase in the cutting rate and a decrease in feed per tooth leads to a decrease in surface roughness. The effect of build-up formation and hence the worst roughness were observed at a cutting rate of 30 m/min and a feed rate of 0.0345 mm/tooth. The minimum achievable roughness of R_a 0.206 μm is achieved at a cutting speed of 65 m/min and at a feed rate of 0.0115 mm/tooth. The material being machined during the cutting process is prone to the formation of burrs on the edges of the workpiece and additional operations are required to remove them. In general, the authors point out that additional research is required to determine the process parameters for the machinability of such steel.

Article [98] presents research findings about the improvement of the surface roughness of maraging nickel steel caused by milling. Steel workpieces were obtained by selective laser melting. The authors point out that roughness R_a decreases from 10 to 0.4 μm after the milling. Also, data on the morphology of material destruction are given by the example

of research on the microstructure of shavings. The use of heat treatment (aging) caused an increase in the components of cutting forces leading to increased cutting tool wear.

The microhardness of sintered stainless steels affects machinability through blade-cutting processes. For example, it was found that the microhardness HV of maraging steel is 40–45% higher than that of chromium-molybdenum steel with the same initial powder particle size [36]. Accordingly, the radial component of the cutting force that emerges during milling also increases by 10–15%. A comparison of similar parameters with cast carbon steel has shown a difference in the microhardness and the radial component of the cutting force by 60% and 20%, respectively.

It was shown in [2] that when steel containing a sufficient amount of martensite is milled after laser sintering, roughness Ra decreases from 22.78 μm to 0.6 μm .

In the process of final turning of 316L steel with the initial roughness Ra of $7 \pm 1 \mu\text{m}$, the authors of [16] managed to consistently obtain Ra below 1 μm . In this case, the thickness of the deformed layer was 10–20 μm , and the microhardness increased by 9–23% as compared to an unturned surface.

Results of studies of the longitudinal turning process of 316L steel obtained by laser alloying are given in [76]. The authors point out that it is feed that has the greatest effect on cutting forces during treatment, and with an increase in the cutting speed, a decrease in the forces is observed. This is explained by an increase in the rate of formation of deformations in the material. Also, an increase in the feed rate leads to increased roughness Ra, and the highest values were obtained at a cutting rate of $\sim 100 \text{ m/min}$. The temperature measured during turning decreases as the feed rate and cutting rate is increased.

Direct pulsed laser deposition from wire and subsequent high-speed milling (i.e., a hybrid process of the fabrication of stainless chromium-nickel steel products) are studied in [66]. Such a sequence of operations was performed on the same combined action equipment. The authors pointed out that this approach allows for creating finished products by reducing the roughness and ensuring dimensional accuracy during milling. That means that, in a single workpiece placement, the output of a finished part is ensured without changing the process base. It was also noted that the use of milling with further material deposition leads to a decrease in the likelihood of porosity and cracks in the workpiece material.

Article [23] presents data on the use of a hybrid process (high-energy laser sintering from powder with subsequent milling) for the production of 316L stainless steel products. An improvement in roughness was observed when milling at low feed rates. Also, a simultaneous increase in the thickness of the cut layer and the feed rate was leading to a deterioration in the quality of the surface layer.

Research work [87] presents data on the possibility of increasing the efficiency of removal of supports by pouring conical supports into solid epoxy resin. This solution has made it possible to reduce the probability of defects through the elimination of bending of supports and the formation of cracks while also reducing the magnitude of the emerging cutting forces.

3.2. Grinding and Abrasive Process

During grinding, local elastic deformations of the abrasive wheel and the workpiece affect the formation of surface roughness. In this case, the properties and structure of the grinding wheel play a leading role, so the deformations of parts during treatment are normally neglected. It is also known that a decrease in roughness during abrasive treatment occurs with an increase in the hardness of the material being processed. This is explained by a decrease in the magnitude of elastic recovery and an increase in normal forces, which provide for an increase in the depth of penetration of abrasive grains into the workpiece during grinding. Studies show that the parameters of the grinding process of AM-fabricated steels can be ranged by the degree of their influence on the roughness: treatment time, hardness and wheel material, grain size (grain size), and depth of cutting.

Article [108] provides data on the use of the magnetic-abrasive treatment process on a 316L steel obtained by laser alloying, an AM technique (Figure 3).

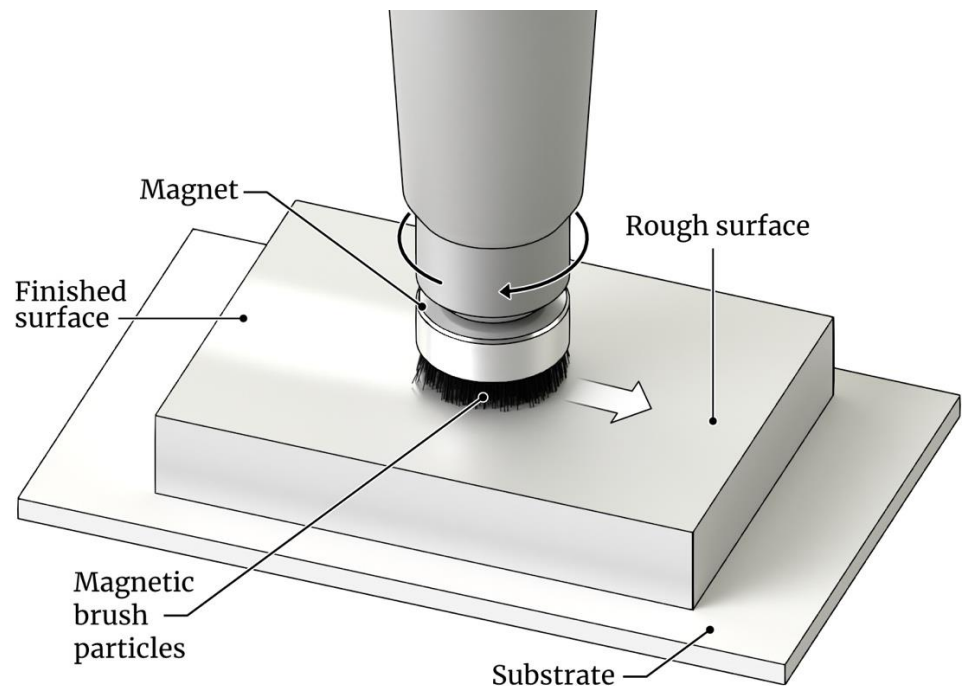


Figure 3. Schematic diagram of the implementation of magnetic-abrasive treatment of a flat surface.

It is pointed out that the technology of magnetic-abrasive treatment effectively removes microdroplets and macrodefects obtained during the crystallization of upper layers in the course of printing. Studies show the dominant influence of the angle of inclination during laser cladding on the formation of surface roughness. The authors also note that the efficiency of the technology is confirmed by measurements of the protrusion height parameter, which can be reduced by more than 2 times by magnetic-abrasive treatment. However, with such treatment, the effect of inheriting a microprofile from the previous surface is observed.

3.3. Tumbling or Treatment in a Free Abrasive Medium

A special case of treatment in a free abrasive environment, tumbling (see Figure 4) can be used on workpieces obtained by AM methods. Tumbling is capable of performing such treatment as cleaning supports after 3D printing, smoothing out microroughnesses as well as dimensionless grinding and polishing. For tumbling, special abrasive bodies of various shapes, sizes, and chemical compositions are used, and they repeatedly collide with the workpiece during treatment. Often, during the tumbling process, the movement of tumbling bodies and workpieces is caused by vibrational, rotational, and combined types of movement. The tumbling process has a distinctive feature: in addition to mechanical removal of material, process kinematics cause the surface layers of the metal to compact thus forming residual compressive stresses. This effect contributes to an increase in fatigue strength, corrosion resistance, and surface microhardness [109,110]. It should be noted that there are virtually no studies devoted to research on the influence of the technological capabilities of tumbling on the characteristics of AM-fabricated 316L steels. That is why the author assumes that the acquisition of such new knowledge is very promising.

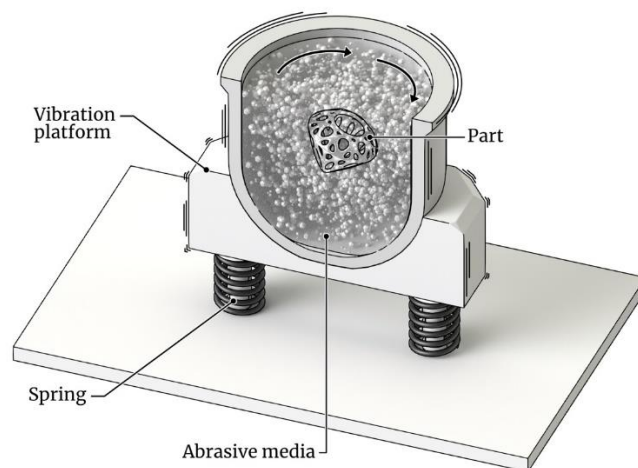


Figure 4. Schematic diagram of the implementation of the vibratory tumbling process in a free abrasive.

3.4. Polishing (Finishing)

The polishing process is considered an operation aimed at reducing and smoothing out workpiece surface roughness. Polishing is normally performed after milling and removal of supports that were required for the growth of the material during printing [88]. In some cases, it is possible to obtain a surface with specular reflection or gloss that is typical of a metal. In addition to the effect of specular reflection, polished surfaces acquire improved characteristics pertinent to the resistance to fatigue failure [68,102]. Also, polished surfaces gain visually appealing properties so they could be used as decorative elements in car interiors, for example.

Polishing can be implemented by mechanical (pastes and soft wheels) and physical treatment methods.

3.5. Chemical Polishing and Electropolishing

Liquid chemical and electrochemical polishing methods are based on the immersion of AM workpieces into baths with chemical solutions with controlled temperature and electric current parameters (see Figure 5). There are small differences in the process duration and medium temperature, which directly affect the depth of material removal. The parameters of chemical polishing, for example, are set to achieve a specular finish and to add a sheen to the metal surface. Chemical treatments are often used to reduce surface roughness ridges and achieve a smooth microprofile. Wet chemical polishing allows both external and internal hard-to-reach surfaces to be treated, which gives it an edge over conventional mechanical polishing methods. This technology is especially often used in the treatment of cavities of tanks for mixing liquids and gases, assemblies of pass-through and thimble ducts, and various cellular structures.

For example, it was shown in [4] that the initial structure of the workpiece surface, the position of the electrode, and the temperature of the electrolyte do not significantly affect the quality of surface polishing, and the achieved value of R_a varies within 10%. However, the authors managed to achieve optimal electrolytic conductivity by lowering electrolyte temperature to 35 °C. The article also shows that with an increase in current and time it is possible to obtain lower R_a values at the cost of a risk of compromising workpiece shape due to excessive material losses.

Article [6] proposes a polishing method using wire. The authors carried out studies on 316L steel and obtained data on a decrease in roughness R_a by more than 3–4 times as compared with the original surface. It was also shown that surface “healing” occurs and it eliminates the artifacts, irregularities, surface voids, and porosity that had been formed during the sintering process.

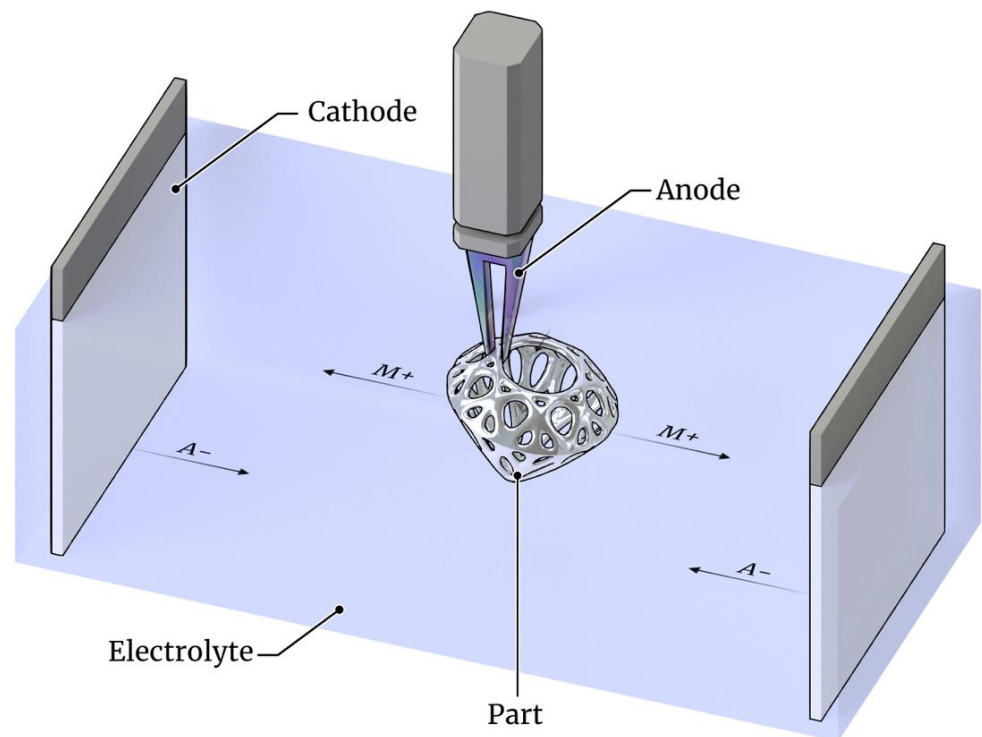


Figure 5. Schematic diagram of the implementation of electropolishing technology in an acidic electrolyte environment.

In article [109], the authors present the results of a study on the reduction of the roughness of the internal surfaces of parts made of an AM-produced 316L steel. Thus, the possibility of a uniform decrease in roughness parameter R_a from 15 to 0.4 μm was determined. It was also found that there is a decrease in parameter R_t by a factor of 20 or more as compared to a surface obtained by AM only. This indicates removal of protruding roughness peaks.

In article [110], the authors used and compared processes of chemical and electrical polishing in order to reduce surface roughness on an AM-produced 316L steel. It is noted that electropolishing provides a smoother surface, while chemical polishing ensures the treatment of even internal cavities and it can significantly reduce roughness.

3.6. Combined Polishing Techniques

Combined polishing techniques include polishing techniques that utilize various radiation sources: laser, electron beam, etc (see Figure 6). Laser radiation is used as a source of generated energy for local micromachining of the surface of workpieces obtained by AM. For implementing such treatment, equipment that is capable of varying radiation wavelength, pulse duration, and waveform is used. The selection of treatment regimes and focusing conditions should ensure the minimization of energy losses while also being sufficient for achieving certain parameters of the surface to be treated. Because of the melt-through of thin surface layers and their subsequent hardening, surface microprofile changes.

In article [40], the authors present data on the study of the process of laser polishing of chromium steel. For polishing, the authors used cycloidal laser beam movement and constant feed rate. In the course of the research, it was found that the penetration depth was 0.204–0.434 mm, and the roughness was reduced by more than 24% of the initial value.

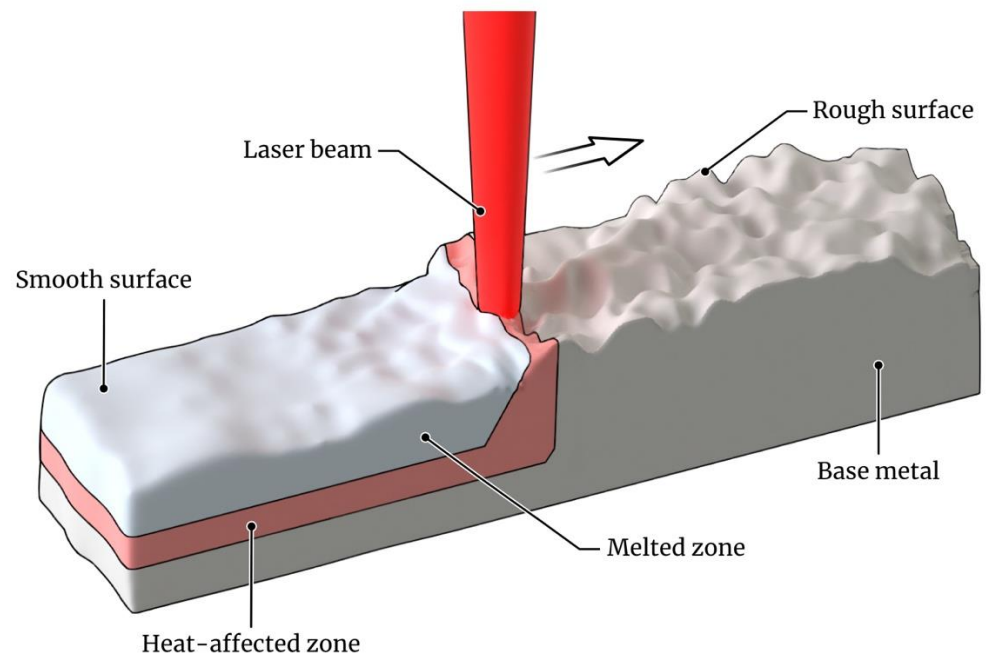


Figure 6. Schematic diagram of the implementation of laser melting of a surface with subsequent polishing at the microprofile level (roughness).

Paper [52] presents the results of a study of surface formation in the course of laser polishing of 316L steel. Due to the micromelting of the surface with a laser beam, a new surface is formed and it differs in the roughness parameters and microstructure which translates into a range of useful mechanical characteristics.

In [14], the authors use Taguchi's statistical methods to plan an experiment aimed to determine the effect of electrochemical polishing parameters on surface roughness. In the research, samples of chromium-nickel steel obtained by laser sintering in layers of 20 μm were used for polishing. As a result, the factors leading to a guaranteed highest possible reduction in roughness to Ra 1.97–2.84 μm were determined.

Articles [52,77] provide data on the use of laser polishing of 316L steel. In this case, the following ranges of roughness reduction are achievable: Ra, from 4.84 to 0.65 μm , Ra, from 10.4 to 2.7 μm .

In [22], the authors present data from experimental research findings on the reduction of the roughness of nickel-cobalt steel obtained by selective laser sintering. It was found that polishing with a continuous-wave laser helps to reduce roughness from Ra 12 to 0.7 μm while a 15% increase in the microhardness of the polished surface is also observed.

Article [109] presents the results of studies on the effect of electrochemical polishing of stainless chromium steel with the addition of abrasive particles to the electrolyte. In the article, information on the optimal composition of a suspension consisting of oxalic acid, hydrogen peroxide, and certain content of silicon oxide is given.

For chemical polishing of workpieces obtained by AM, innovative methods are also used that compete with conventional liquid-based ones. A key feature of the DLYte[®] method described in [109,110] is the use of dry granules consisting of a strong acid cation exchanger (CAS No. 69011-20-7) and a small amount of sulfuric acid (<1.0% weight), followed by supplying a minimum amount of distilled water and electric current to the treatment zone whereby the duration and frequency of voltage and pulses are also varied. The workpieces are moved by actuating holders movement in two planes along the trajectory of the cam mechanism, and the working medium is moved by vibrations.

A humid environment provides for monitoring and adjusting the intensity of the polishing process, which is achieved by varying the electrical conductivity of the workpiece surface. Stainless steel treatment after AM results in the formation of a uniform surface

morphology without traces of cracking, which are usually characteristic of liquid electrochemical treatment. The time for DLyte[®] polishing may vary between 0.5 and 6 h in order to reduce roughness Ra from $8.72 \pm 0.35 \mu\text{m}$ to $0.75 \pm 0.08 \mu\text{m}$. Meanwhile, a study [110] shows that the intensity of the removal of material from 316L steel and reduction in the roughness of the workpiece surface facing the bottom of the container increases by 30–35% as compared to its side surface. This circumstance is important, especially when designing a treatment process for mission-critical products.

4. Conclusions

This article discusses the technological solutions for AM-manufactured stainless steels. Based on the analysis of a number of publications, the properties of the surface morphology and physical and mechanical characteristics achieved in the process of obtaining workpieces were singled out. It was pointed out that the use of workpieces as full-fledged functional products is impossible due to low surface quality and the inability of ensuring physical and mechanical properties without post-processing. By adjusting the processes and regimes of post-processing and thermal treatment, it is possible to control the properties of the structure and surface morphology of AM-produced stainless steel. From scientific research experience and research findings in various publications, we can summarize the need to use both conventional and combined post-processing techniques, aimed at predicting the behavior of functional products in various assemblies and components.

Author Contributions: Conceptualization, A.B. and V.P.; validation, N.S., A.S. and V.B.; formal analysis, A.V.; data curation, A.B.; writing—original draft preparation, A.B.; writing—review and editing, V.P.; visualization, A.V. All authors have read and agreed to the published version of the manuscript.

Funding: This research was supported by The Ministry of Science and Higher Education of the Russian Federation (Agreement No 075-15-2020-785 dated 23 September 2020).

Data Availability Statement: Not applicable.

Conflicts of Interest: The authors declare no conflict of interest.

References

1. Sreehitha, V. Impact of 3D printing in the automotive industry. *Int. J. Mech. Prod. Eng.* **2017**, *5*, 91–94.
2. Bai, Y.; Chaudhari, A.; Wang, H. Investigation on the microstructure and machinability of ASTM A131 steel manufactured by directed energy deposition. *J. Mater. Process. Technol.* **2020**, *276*, 116410. [[CrossRef](#)]
3. Makinen, M.; Jauhiainen, E.; Matilainen, V.; Riihimäki, J.; Ritvanen, J.; Piili, H.; Salminen, A. Preliminary Comparison of Properties between Ni-electroplated Stainless Steel Parts Fabricated with Laser Additive Manufacturing and Conventional Machining. *Phys. Procedia* **2015**, *78*, 337–346. [[CrossRef](#)]
4. Núñez, P.J.; García-Plaza, E.; Hernando, M.; Trujillo, R. Characterization of Surface Finish of Electropolished Stainless Steel AISI 316L with Varying Electrolyte Concentrations. *Procedia Eng.* **2013**, *63*, 771–778. [[CrossRef](#)]
5. Hällgren, S.; Pejryd, L.; Ekengren, J. Additive Manufacturing and High Speed Machining-cost Comparison of short Lead Time Manufacturing Methods. *Procedia CIRP* **2016**, *50*, 384–389. [[CrossRef](#)]
6. Boban, J.; Ahmed, A.; Rahman, M.A.; Rahman, M. Wire electrical discharge polishing of additive manufactured metallic components. *Procedia CIRP* **2020**, *87*, 321–326. [[CrossRef](#)]
7. Parenti, P.; Cataldo, S.; Grigis, A.; Covelli, M.; Annoni, M. Implementation of hybrid additive manufacturing based on extrusion of feedstock and milling. *Procedia Manuf.* **2019**, *34*, 738–746. [[CrossRef](#)]
8. Langi, E.; Bisht, A.; Silberschmidt, V.V.; Ruiz, P.D.; Vogt, F.; Mailto, L.; Masseling, L.; Zhao, L. Characterisation of Additively Manufactured Metallic Stents. *Procedia Struct. Integr.* **2019**, *15*, 41–45. [[CrossRef](#)]
9. Rotty, C.; Mandroyan, A.; Doche, M.L.; Monney, S.; Hihn, J.Y.; Rouge, N. Electrochemical Superfinishing of Cast and ALM 316L Stainless Steels in Deep Eutectic Solvents: Surface Microroughness Evolution and Corrosion Resistance. *J. Electrochem. Soc.* **2019**, *166*, 468. [[CrossRef](#)]
10. Fousová, M.; Vojtěch, D.; Kubásek, J.; Dvorský, D.; Machová, M. 3D Printing as an Alternative to Casting, Forging and Machining Technologies? *Manuf. Technol.* **2015**, *15*, 809–814. [[CrossRef](#)]
11. Gu, D.D.; Meiners, W.; Poprawe, R. Laser additive manufacturing of metallic components: Materials, processes and mechanisms. *Int. Mater. Rev.* **2012**, *57*, 133–164. [[CrossRef](#)]
12. Tilton, M.; Lewis, G.S.; Manogharan, G.P. Additive Manufacturing of Orthopedic Implants. In *Orthopedic Biomaterials*; Springer: Cham, Switzerland, 2018; pp. 21–55.

13. Adekanye, S.A.; Mahamood, R.M.; Akinlabi, E.T.; Owolabi, M.G. Additive manufacturing: The future of manufacturing. *Addit. Manuf.* **2017**, *709*, 715. [[CrossRef](#)]
14. Brent, D.; Saunders, T.A.; Moreno, F.G.; Tyagi, P. Taguchi Design of Experiment for the Optimization of Electrochemical Polishing of Metal Additive Manufacturing Components. *ASME Int. Mech. Eng. Congr. Expo.* **2016**, 50527, V002T02A014.
15. Traxel, K.D.; Bandyopadhyay, A. First demonstration of additive manufacturing of cutting tools using directed energy deposition system: Stellite™-based cutting tools. *Addit. Manuf.* **2019**, *25*, 460–468. [[CrossRef](#)]
16. Kaynak, Y.; Kitay, O. Porosity, surface quality, microhardness and microstructure of selective laser melted 316L stainless steel resulting from finish machining. *J. Manuf. Mater. Process.* **2018**, *2*, 36. [[CrossRef](#)]
17. Teo, A.Q.A.; Yan, L.; Chaudhari, A.; O'Neill, G.K. Post-processing and surface characterization of additively manufactured stainless steel 316l lattice: Implications for biomedical use. *Materials* **2021**, *14*, 1376. [[CrossRef](#)]
18. Batista, C.D.; das Neves de Pinho Fernandes, A.A.M.; Vieira, M.T.F.; Emadina, O. From Machining Chips to Raw Material for Powder Metallurgy—A Review. *Materials* **2021**, *14*, 5432. [[CrossRef](#)]
19. Popov, V.V.; Fleisher, A. Hybrid additive manufacturing of steels and alloys. *Manuf. Rev.* **2020**, *7*, 6. [[CrossRef](#)]
20. Kozior, T.; Bochnia, J. The influence of printing orientation on surface texture parameters in powder bed fusion technology with 316L steel. *Micromachines* **2020**, *11*, 639. [[CrossRef](#)]
21. Aqilah, D.N.; Sayuti, M.; Yusof, F.; Dambatta, Y.; Amran, N.A.M.; Izzati, W.N. Effects of process parameters on the surface roughness of stainless steel 316L parts produced by selective laser melting. *J. Test. Eval.* **2018**, *46*, 1673–1683. [[CrossRef](#)]
22. Yung, K.C.; Zhang, S.S.; Duan, L.; Choy, H.S.; Cai, Z.X. Laser polishing of additive manufactured tool steel components using pulsed or continuous-wave lasers. *Int. J. Adv. Manuf. Technol.* **2019**, *105*, 425–440. [[CrossRef](#)]
23. Yang, Y.; Gong, Y.; Qu, S.; Xie, H.; Cai, M.; Xu, Y. Densification, mechanical behaviors, and machining characteristics of 316L stainless steel in hybrid additive/subtractive manufacturing. *Int. J. Adv. Manuf. Technol.* **2020**, *107*, 177–189. [[CrossRef](#)]
24. Lu, Y.; Sun, G.F.; Wang, Z.D.; Su, B.Y.; Zhang, Y.K.; Ni, Z.H. The effects of laser peening on laser additive manufactured 316L steel. *Int. J. Adv. Manuf. Technol.* **2020**, *107*, 2239–2249. [[CrossRef](#)]
25. Jeng, J.Y.; Lin, M.C. Mold fabrication and modification using hybrid processes of selective laser cladding and milling. *J. Mater. Process. Technol.* **2001**, *110*, 98–103. [[CrossRef](#)]
26. Brown, D.W.; Losko, A.; Carpenter, J.S.; Cooley, J.C.; Clausen, B.; Dahal, J.; Kenesei, P.; Park, J.S. Microstructure development of 308L stainless steel during additive manufacturing. *Metall. Mater. Trans. A* **2019**, *50*, 2538–2553. [[CrossRef](#)]
27. Marya, M.; Singh, V.; Marya, S.; Hascoet, J.Y. Microstructural development and technical challenges in laser additive manufacturing: Case study with a 316L industrial part. *Metall. Mater. Trans. B* **2015**, *46*, 1654–1665. [[CrossRef](#)]
28. Riemer, A.; Leuders, S.; Thone, M.; Richard, H.A.; Troster, T.; Niendorf, T. On the fatigue crack growth behavior in 316L stainless steel manufactured by selective laser melting. *Eng. Fract. Mech.* **2014**, *120*, 15–25. [[CrossRef](#)]
29. Kumbhar, N.N.; Mulay, A.V. Post processing methods used to improve surface finish of products which are manufactured by additive manufacturing technologies: A review. *J. Inst. Eng. Ser. C* **2018**, *99*, 481–487. [[CrossRef](#)]
30. Sireesha, M.; Lee, J.; Kiran, A.S.K.; Babu, V.J.; Kee, B.B.T.; Ramakrishna, A. A review on additive manufacturing and its way into the oil and gas industry. *RSC Adv.* **2018**, *8*, 22460–22468. [[CrossRef](#)]
31. Horn, T.J.; Harrysson, O.L.A. Overview of current additive manufacturing technologies and selected applications. *Sci. Prog.* **2012**, *95*, 255–282. [[CrossRef](#)]
32. Spierings, A.B.; Starr, T.L.; Wegener, K. Fatigue performance of additive manufactured metallic parts. *Rapid Prototyp. J.* **2013**, *19*, 88–94. [[CrossRef](#)]
33. Örnek, C. Additive manufacturing—A general corrosion perspective. *Corros. Eng. Sci. Technol.* **2018**, *53*, 531–535. [[CrossRef](#)]
34. Zhukov, V.V.; Grigorenko, G.M.; Shapovalov, V.A. Additive manufacturing of metal products. *Paton Weld. J.* **2016**, *5*, 137–142. [[CrossRef](#)]
35. Song, Y.A.; Park, S.; Choi, D.; Jee, H. 3D welding and milling: Part I—A direct approach for freeform fabrication of metallic prototypes. *Int. J. Mach. Tools Manuf.* **2005**, *45*, 1057–1062. [[CrossRef](#)]
36. Strano, G.; Hao, L.; Everson, R.M.; Evans, K.E. Surface roughness analysis, modelling and prediction in selective laser melting. *J. Mater. Process. Technol.* **2013**, *213*, 589–597. [[CrossRef](#)]
37. Luecke, W.E.; Slotwinski, J.A. Mechanical properties of austenitic stainless steel made by additive manufacturing. *J. Res. Natl. Inst. Stand. Technol.* **2014**, *119*, 398. [[CrossRef](#)]
38. Urhal, P.; Weightman, A.; Diver, C.; Bartolo, P. Robot assisted additive manufacturing: A review. *Robot. Comput. Integr. Manuf.* **2019**, *59*, 335–345. [[CrossRef](#)]
39. Nowotny, S.; Scharek, S.; Beyer, E.; Richter, K.H. Laser beam build-up welding: Precision in repair, surface cladding, and direct 3D metal deposition. *J. Therm. Spray Technol.* **2007**, *16*, 344–348. [[CrossRef](#)]
40. Caggiano, A.; Teti, R.; Alfieri, V.; Caiazza, F. Automated laser polishing for surface finish enhancement of additive manufactured components for the automotive industry. *Prod. Eng.* **2021**, *15*, 109–117. [[CrossRef](#)]
41. Mohd, Y.S.; Cutler, S.; Gao, N. The impact of metal additive manufacturing on the aerospace industry. *Metals* **2019**, *9*, 1286. [[CrossRef](#)]
42. Habibzadeh, S.; Li, L.; Shum-Tim, D.; Davis, E.C.; Omanovic, S. Electrochemical polishing as a 316L stainless steel surface treatment method: Towards the improvement of biocompatibility. *Corros. Sci.* **2014**, *87*, 89–100. [[CrossRef](#)]

43. Du, W.; Bai, Q.; Zhang, B. A novel method for additive/subtractive hybrid manufacturing of metallic parts. *Procedia Manuf.* **2016**, *5*, 1018–1030. [[CrossRef](#)]
44. Cao, J.; Brinksmeier, E.; Fu, M.; Gao, R.X.; Liang, B.; Merklein, M.; Schmidt, M.; Yanagimoto, J. Manufacturing of advanced smart tooling for metal forming. *CIRP Ann.* **2019**, *68*, 605–628. [[CrossRef](#)]
45. Trojan, K.; Ocelík, V.; Čapek, J.; Čech, J.; Canelo-Yubero, D.; Ganev, N.; Kolařík, K.; De Hosson, J.T.M. Microstructure and Mechanical Properties of Laser Additive Manufactured H13 Tool Steel. *Metals* **2022**, *12*, 243. [[CrossRef](#)]
46. Liu, G.; Zhang, X.; Chen, X.; He, Y.; Cheng, L.; Huo, M.; Yin, J.; Hao, F.; Chen, S.; Wang, P.; et al. Additive manufacturing of structural materials. *Mater. Sci. Eng. R Rep.* **2021**, *145*, 100596. [[CrossRef](#)]
47. Korium, M.S.; Roozbahani, H.; Alizadeh, M.; Perepelkina, S.; Handroos, H. Direct Metal Laser Sintering of Precious Metals for Jewelry Applications: Process Parameter Selection and Microstructure Analysis. *IEEE Access* **2021**, *9*, 126530–126540. [[CrossRef](#)]
48. Skrzyniarz, M.; Nowakowski, L.; Blasiak, S. Geometry, Structure and Surface Quality of a Maraging Steel Milling Cutter Printed by Direct Metal Laser Melting. *Materials* **2022**, *15*, 773. [[CrossRef](#)] [[PubMed](#)]
49. Leicht, A.; Klement, U.; Hryha, E. Effect of build geometry on the microstructural development of 316L parts produced by additive manufacturing. *Mater. Charact.* **2018**, *143*, 137–143. [[CrossRef](#)]
50. Yuan, X.; Guo, X.; Qiu, H.; Cui, F.; Wang, X.; Guan, N.; Li, H.; Li, J.; Zhan, J.; Zeng, F. Mechanical Properties and Microstructure of 316 Stainless Steel Processed by Pulsed Micro-Plasma Additive Manufacturing. *J. Therm. Spray Technol.* **2022**, *31*, 623–635. [[CrossRef](#)]
51. Zhang, X.; Cui, W.; Li, W.; Liou, F. A Hybrid Process Integrating Reverse Engineering, Pre-Repair Processing, Additive Manufacturing, and Material Testing for Component Remanufacturing. *Materials* **2019**, *12*, 1961. [[CrossRef](#)]
52. Lopes, J.G.; Machado, C.M.; Duarte, V.R.; Rodrigues, T.A.; Santos, T.G.; Oliveria, J.P. Effect of milling parameters on HSLA steel parts produced by Wire and Arc Additive Manufacturing (WAAM). *J. Manuf. Process.* **2020**, *59*, 739–749. [[CrossRef](#)]
53. Khan, H.M.; Karabulut, Y.; Kitay, O.; Kaynak, Y.; Jawahir, I.S. Influence of the post-processing operations on surface integrity of metal components produced by laser powder bed fusion additive manufacturing: A review. *Mach. Sci. Technol.* **2020**, *25*, 118–176. [[CrossRef](#)]
54. Boyard, N. Design for Additive Manufacturing—DFAM. *J. Mater. Process. Technol.* **2014**, *12*, 616–622.
55. Liu, Y.; Zhang, M.; Shi, W.; Ma, Y.; Yang, J. Study on performance optimization of 316L stainless steel parts by High-Efficiency Selective Laser Melting. *Opt. Laser Technol.* **2021**, *138*, 106872. [[CrossRef](#)]
56. Yadroitsev, I.; Yadroitsava, I. Evaluation of residual stress in stainless steel 316L and Ti6Al4V samples produced by selective laser melting. *Virtual Phys. Prototyp.* **2015**, *10*, 67–76. [[CrossRef](#)]
57. Wu, A.S.; Brown, D.W.; Kumar, M.; Gallegos, G.F.; King, W.E. An experimental investigation into additive manufacturing-induced residual stresses in 316L stainless steel. *Metall. Mater. Trans. A* **2014**, *45*, 6260–6270. [[CrossRef](#)]
58. Yadollahi, A.; Shamsaei, N.; Thompson, S.M.; Seely, D.W. Effects of process time interval and heat treatment on the mechanical and microstructural properties of direct laser deposited 316L stainless steel. *Mater. Sci. Eng. A* **2015**, *644*, 171–183. [[CrossRef](#)]
59. Trelewicz, J.R.; Halada, G.P.; Donaldson, O.K.; Manoghran, G. Microstructure and corrosion resistance of laser additively manufactured 316L stainless steel. *JOM* **2016**, *68*, 850–859. [[CrossRef](#)]
60. Cherry, J.A.; Davies, H.M.; Mehmood, S.; Lavery, N.P.; Brown, S.G.R.; Sienz, J. Investigation into the effect of process parameters on microstructural and physical properties of 316L stainless steel parts by selective laser melting. *Int. J. Adv. Manuf. Technol.* **2015**, *76*, 869–879. [[CrossRef](#)]
61. Ziętała, M.; Durejko, T.; Polański, M.; Kuncze, I.; Płociński, T.; Zieliński, W.; Łazińska, M.; Stępniewski, W.; Czujko, T.; Kurzydowski, K.J.; et al. The microstructure, mechanical properties and corrosion resistance of 316 L stainless steel fabricated using laser engineered net shaping. *Mater. Sci. Eng. A* **2016**, *677*, 1–10. [[CrossRef](#)]
62. Portella, Q.; Chemkhi, M.; Reira, D. Influence of surface mechanical attrition treatment (SMAT) post-treatment on microstructural, mechanical and tensile behaviour of additive manufactured AISI 316L. *Mater. Charact.* **2020**, *167*, 110463. [[CrossRef](#)]
63. Zhang, B.; Dembinski, L.; Coddet, C. Materials Science & Engineering A The study of the laser parameters and environment variables effect on mechanical properties of high compact parts elaborated by selective laser melting 316L powder. *Mater. Sci. Eng. A* **2013**, *584*, 21–31.
64. Dirisu, P.; Ganguly, D.; Mehmanparast, A.; Martina, F.; Williams, S. Analysis of fracture toughness properties of wire+ arc additive manufactured high strength low alloy structural steel components. *Mater. Sci. Eng. A* **2019**, *765*, 138285. [[CrossRef](#)]
65. Yao, C.; Xiaotong, P.; Qunfu, G.; Zhijie, W.; Pulin, N. Effect of laser remelting on the microstructure and mechanical properties of AerMet100 steel fabricated by laser cladding. *Mater. Sci. Eng. A* **2022**, *840*, 142951. [[CrossRef](#)]
66. Ye, Z.; Zhang, Z.; Jin, Z.; Xiao, M.; Su, J. Study of hybrid additive manufacturing based on pulse laser wire depositing and milling. *Int. J. Adv. Manuf. Technol.* **2017**, *88*, 2237–2248. [[CrossRef](#)]
67. Mirzababaei, S.; Pasebani, S. A review on binder jet additive manufacturing of 316L stainless steel. *J. Manuf. Mater. Process.* **2019**, *3*, 82. [[CrossRef](#)]
68. F2792-12a; Standard terminology for additive manufacturing technologies. ASTM International: West Conshohocken, PA, USA, 2012.
69. He, X.; Mazumder, J. Transport phenomena during direct metal deposition. *J. Appl. Phys.* **2007**, *101*, 053113. [[CrossRef](#)]

70. Kučerová, L.; Burdova, K.; Jenicek, S.; Chena, I. Effect of solution annealing and precipitation hardening at 250 C–550 C on microstructure and mechanical properties of additively manufactured 1.2709 maraging steel. *Mater. Sci. Eng. A* **2021**, *814*, 141195. [[CrossRef](#)]
71. Mooney, B.; Kourousis, K.I.; Raghavendra, R. Plastic anisotropy of additively manufactured maraging steel: Influence of the build orientation and heat treatments. *Addit. Manuf.* **2019**, *25*, 19–31. [[CrossRef](#)]
72. Islam, N.K.M.S.; Harun, W.S.W.; Ghani, S.A.C.; Omar, M.A.; Ramli, M.H.; Ismail, M.H. Physical properties and microstructure study of stainless steel 316L alloy fabricated by selective laser melting. *AIP Conf. Proc.* **2017**, *1901*, 100015.
73. Mercelis, P. Binding mechanisms in selective laser sintering and selective laser melting. *Rapid Prototyp. J.* **2005**, *11*, 26–36.
74. Klotz, U.E.; Tiberto, D.; Held, F.; Klotz, U.E.; Tiberto, D.; Held, F. Additive manufacturing of 18-karat yellow-gold alloys. In Proceedings of the Santa Fe Symposium on Jewelry Manufacturing Technology, Santa Fe, NM, USA, 15–18 May 2016; pp. 255–272.
75. Yin, S.; Yan, X.; Jenkins, R.; Chen, C.; Kazasidis, M.; Liu, M.; Kuang, M.; Lupoi, R. Hybrid additive manufacture of 316L stainless steel with cold spray and selective laser melting: Microstructure and mechanical properties. *J. Mater. Process. Technol.* **2019**, *273*, 116248. [[CrossRef](#)]
76. Struzikiewicz, G.; Zębala, W.; Matras, A.; Machno, M.; Ślusarczyk, Ł.; Hichert, S.; Laufer, F. Turning Research of Additive Laser Moltien Stainless Steel 316L Obtained by 3D Printing. *Materials* **2019**, *12*, 182. [[CrossRef](#)] [[PubMed](#)]
77. Obeidi, M.A.; McCarthy, E.; O’Connell, B.; Ul Ahad, I.; Brabazon, D. Laser Polishing of Additive Manufactured 316L Stainless Steel Synthesized by Selective Laser Melting. *Materials* **2019**, *12*, 991. [[CrossRef](#)] [[PubMed](#)]
78. Lutter-Günther, M.; Wagner, S.; Seidel, C.; Reinhart, G. Economic and ecological evaluation of hybrid additive manufacturing technologies based on the combination of laser metal deposition and CNC machining. *Appl. Mech. Mater.* **2015**, *805*, 213–222. [[CrossRef](#)]
79. Gadelmawla, E.S.; Koura, M.M.; Maksoud, T.M.A.; Elwa, I.M.; Soliman, H.H. Roughness parameters. *J. Mater. Process. Technol.* **2002**, *123*, 133–145. [[CrossRef](#)]
80. Helmlí, F.; Pötsch, K.; Repitsch, C. Choosing the appropriate parameter. In *Characterisation of Areal Surface Texture*; Springer: Berlin/Heidelberg, Germany, 2013; pp. 155–177.
81. Yadroitsev, I.; Smurov, I. Surface morphology in selective laser melting of metal powders. *Phys. Procedia* **2011**, *12*, 264–270. [[CrossRef](#)]
82. Yang, L.; Laugel, N.; Housden, I.; Espitlier, L.; Matthews, A.; Yerokhin, A. Plasma additive layer manufacture smoothing (PALMS) technology—An industrial prototype machine development and a comparative study on both additive manufactured and conventional machined AISI 316 stainless steel. *Addit. Manuf.* **2020**, *34*, 101204. [[CrossRef](#)]
83. Zhang, Z.; Li, Z.; He, Y.; Song, G.; Liu, L. The effect of low-power laser on micro-forming of 316 stainless steel additive manufacturing part. *J. Manuf. Processes* **2021**, *68*, 583–601. [[CrossRef](#)]
84. Williams, S.W. Wire+ arc additive manufacturing. *Mater. Sci. Technol.* **2016**, *32*, 641–647. [[CrossRef](#)]
85. Xiong, J.; Lei, Y.; Chen, H.; Zhang, G. Fabrication of inclined thin-walled parts in multi-layer single-pass GMAW-based additive manufacturing with flat position deposition. *J. Mater. Process. Technol.* **2017**, *240*, 397–403. [[CrossRef](#)]
86. Chaturvedi, M.; Scutelnicu, E.; Rusu, C.C.; Mistodie, L.R.; Mihailescu, D.; Subbiah, A.V. Wire Arc Additive Manufacturing: Review on Recent Findings and Challenges in Industrial Applications and Materials Characterization. *Metals* **2021**, *11*, 939. [[CrossRef](#)]
87. Cao, Q.; Shi, Z.; Bai, Y.; Zhang, J.; Zhao, C.; Fuh, J.; Wang, H. A novel method to improve the removability of cone support structures in selective laser melting of 316L stainless steel. *J. Alloys Compd.* **2021**, *854*, 157133. [[CrossRef](#)]
88. Hildreth, O.J.; Nassar, A.R.; Chasse, K.R.; Simpson, T.W. Dissolvable metal supports for 3D direct metal printing. *3d Print. Addit. Manuf.* **2016**, *3*, 90–97. [[CrossRef](#)]
89. Zhang, J.; Lee, Y.J.; Wang, H. A Brief Review on the Enhancement of Surface Finish for Metal Additive Manufacturing. *J. Miner. Met. Mater. Eng.* **2021**, *7*, 1–14.
90. Stepanov, G.A. The Strength of AISI 304L Rolled Sheet Steel with Thickness up to 25 mm. *Chem. Pet. Eng.* **2005**, *41*, 287–290. [[CrossRef](#)]
91. Du, W.; Bai, Q.; Zhang, B. Machining characteristics of 18Ni-300 steel in additive/subtractive hybrid manufacturing. *Int. J. Adv. Manuf. Technol.* **2018**, *95*, 2509–2519. [[CrossRef](#)]
92. Pace, M.L.; Guarnaccio, A.; Dilce, P.; Molica, D.; Parisi, D.P.; Lettino, A.; Medici, L.; Summa, V.; Ciancio, R.; Santagata, A. 3D additive manufactured 316L components microstructural features and changes induced by working life cycles. *Appl. Surf. Sci.* **2017**, *418*, 437–445. [[CrossRef](#)]
93. Ashouri, D.; Voshage, M.; Burkamp, K.; Kunz, J.; Bezold, A.; Schleifenbaum, J.H.; Broeckmann, C. Mechanical behaviour of additive manufactured 316L f2ccz lattice structure under static and cyclic loading. *Int. J. Fatigue* **2020**, *134*, 105503. [[CrossRef](#)]
94. Saeidi, K.; Gao, X.; Lofaj, F.; Kvetkova, L.; Shen, Z.J. Transformation of austenite to duplex austenite-ferrite assembly in annealed stainless steel 316L consolidated by laser melting. *J. Alloys Compd.* **2015**, *633*, 463–469. [[CrossRef](#)]
95. Maleki, E.; Bagherifard, S.; Bandini, M.; Guagliano, M. Surface post-treatments for metal additive manufacturing: Progress, challenges, and opportunities. *Addit. Manuf.* **2021**, *37*, 101619. [[CrossRef](#)]
96. Guenther, E.; Kahlert, M.; Vollmer, M.; Niendorf, T.; Greiner, C. Tribological Performance of Additively Manufactured AISI H13 Steel in Different Surface Conditions. *Materials* **2021**, *14*, 928. [[CrossRef](#)] [[PubMed](#)]

97. Merklein, M.; Plettke, R.; Junker, D.; Schaub, A.; Ahuja, B. Mechanical Testing of Additive Manufactured Metal Parts. *Key Eng. Mater.* **2015**, *651*, 713–718. [[CrossRef](#)]
98. Łyczkowska-Widłak, E.; Lochyński, P.; Nawrat, G. Electrochemical Polishing of Austenitic Stainless Steels. *Materials* **2020**, *13*, 2557. [[CrossRef](#)]
99. Kozhukhova, N.; Kozhukhova, M.; Zhernovskaya, I.; Promakhov, V. The Correlation of Temperature-Mineral Phase Transformation as a Controlling Factor of Thermal and Mechanical Performance of Fly Ash-Based Alkali-Activated Binders. *Materials* **2020**, *13*, 5181. [[CrossRef](#)] [[PubMed](#)]
100. Bai, Y.; Zhao, C.; Yang, J.; Hong, R.; Weng, C.; Wang, H. Microstructure and machinability of selective laser melted high-strength maraging steel with heat treatment. *J. Mater. Process. Technol.* **2021**, *288*, 116906. [[CrossRef](#)]
101. Croccolo, D.; De Agostinis, M.; Fini, S.; Olmi, G.; Robusto, F.; Kostić, S.Ć.; Vranić, A.; Bogojević, N. Fatigue Response of As-Built DMLS Maraging Steel and Effects of Aging, Machining, and Peening Treatments. *Metals* **2018**, *8*, 505. [[CrossRef](#)]
102. Zhao, C.; Bai, Y.; Zhang, Y.; Wang, X.; Xue, J.; Wang, H. Influence of scanning strategy and building direction on microstructure and corrosion behaviour of selective laser melted 316L stainless steel. *Mater. Des.* **2021**, *209*, 109999. [[CrossRef](#)]
103. Jabir, H.A.; Abid, S.R.; Murali, G.; Ali, S.H.; Klyuev, S.; Fediuk, R.; Vatin, N.; Promakhov, V.; Vasilev, Y. Experimental Tests and Reliability Analysis of the Cracking Impact Resistance of UHPFRC. *Fibers* **2020**, *8*, 74. [[CrossRef](#)]
104. Zhukov, I.A.; Kozulin, A.A.; Khrustalyov, A.P.; Matveev, A.E.; Platov, V.V.; Vorozhtsov, A.B.; Zhukova, T.V.; Promakhov, V.V. The Impact of Particle Reinforcement with Al₂O₃, TiB₂, and TiC and Severe Plastic Deformation Treatment on the Combination of Strength and Electrical Conductivity of Pure Aluminum. *Metals* **2019**, *9*, 65. [[CrossRef](#)]
105. Promakhov, V.; Zhukov, A.; Dubkova, Y.; Zhukov, I.; Kovalchuk, S.; Zhukova, T.; Olisov, A.; Klimenko, V.; Savkina, N. Structure and Properties of ZrO₂-20%Al₂O₃ Ceramic Composites Obtained Using Additive Technologies. *Materials* **2018**, *11*, 2361. [[CrossRef](#)] [[PubMed](#)]
106. Artyukhova, N.; Anikeev, S.; Promakhov, V.; Korobekov, M. The Effect of Cobalt on the Deformation Behaviour of a Porous TiNi-Based Alloy Obtained by Sintering. *Materials* **2021**, *14*, 7584. [[CrossRef](#)]
107. Promakhov, V.; Zhukov, A.; Ziatdinov, M.; Zhukov, I.; Schulz, N.; Kovalchuk, S.; Dubkova, Y.; Korsmik, R.; Klimova-Korsmik, O.; Turichin, G.; et al. Inconel 625/TiB₂ Metal Matrix Composites by Direct Laser Deposition. *Metals* **2019**, *9*, 141. [[CrossRef](#)]
108. Mendagaliev, R.; Klimova-Korsmik, O.; Promakhov, V.; Schulz, N.; Zhukov, A.; Klimenko, V.; Olisov, A. Heat Treatment of Corrosion Resistant Steel for Water Propellers Fabricated by Direct Laser Deposition. *Materials* **2020**, *13*, 2738. [[CrossRef](#)] [[PubMed](#)]
109. Promakhov, V.V.; Khmeleva, M.G.; Zhukov, I.A.; Platov, V.V.; Khrustalyov, A.P.; Vorozhtsov, A.B. Influence of Vibration Treatment and Modification of A356 Aluminum Alloy on Its Structure and Mechanical Properties. *Metals* **2019**, *9*, 87. [[CrossRef](#)]
110. Matveev, A.; Promakhov, V.; Schultz, N.; Vorozhtsov, A. Synthesis of Metal Matrix Composites Based on CrxNiy-TiN for Additive Technology. *Materials* **2021**, *14*, 5914. [[CrossRef](#)]